Application of the MAT 213 Composite Impact Model to NASA Problems of Interest

Robert K. Goldberg[1], Trenton M. Ricks[1], Troy Lyons[1], Javier Buenrostro[1], Jacob Putnam[2], Daniel Slaughter[3]

[1]NASA Glenn Research Center, Cleveland, Ohio
[2]NASA Langley Research Center, Hampton, Virginia
[3]Iowa State University, Ames, Iowa

1 Introduction

As composite materials are gaining increased use in aircraft components where impact resistance under high-energy impact conditions is important (such as the turbine engine fan case), the need for accurate material models to simulate the deformation, damage, and failure response of polymer matrix composites under impact conditions is becoming more critical.

While there have been several material models available within LS-DYNA® to analyze the impact response of composites for many years, approximately twelve years ago areas were identified where the predictive capabilities of the models that existed at that time could be improved. These limitations were extensively discussed by Goldberg et al. [1]. One major limitation of the existing models was that the inputs to these models generally consisted of point-wise properties (such as the modulus, failure stress or failure strain in a particular coordinate direction) that led to curve fit approximations to the material stress-strain curves and simplified approximations to the actual material failure surfaces. This type of approach resulted in models with only a few parameters, which provided a crude approximation at best to the actual material response, or in models with many parameters, which required a large number of complex tests to characterize. An alternative approach was developed in which tabulated data, obtained from a well-defined set of physically meaningful experiments, was used. Using tabulated data allowed the actual material response data to be entered in a discretized form, which permitted a more accurate representation of the actual material response. This composite material model, which incorporated deformation, damage and failure has been developed and implemented for use within LS-DYNA and has been given the formal name of *MAT_COMPOSITE_TABULATED_PLASTICITY_DAMAGE as well as the numerical identifier MAT_213. The material model is meant to be a fully generalized model suitable for use with a large number of composite architectures (laminated or textile).

Personnel from the National Aeronautics and Space Administration (NASA), specifically the NASA Glenn Research Center, were extensively involved in the development of MAT_213. However, in recent years the emphasis at NASA has transitioned from development to the utilization of MAT_213 for the analysis of the impact, crush, and crash response of composite structures related to specific applications of interest to NASA projects. In this paper, a representative sample of these efforts will be described. First, a summary of the key features of the MAT_213 material model will be provided. Afterwards, analysis studies related to the crush response of a material suitable for use as a structural energy absorber, the ballistic impact response of a material suitable for use in a rotorcraft fuselage structure, and the impact and damage response of a representative thermoplastic matrix composite material will be described.

2 Summary of MAT_213 Composite Impact Model

The MAT_213 composite impact model consists of a deformation model, a damage model, and a failure model. The deformation model, described extensively in Goldberg et al. [1] and Hoffarth, et al. [2] is based on modifying the equations used for the Tsai-Wu composite failure model [3] to serve as a strain hardening plasticity model with a non-associative flow rule. For the damage model, described extensively in Goldberg et al. [4], a strain equivalent formulation is used where the total, elastic and plastic strains are the same in the equivalent undamaged state as in the damaged state. This equivalence allows the deformation and damage calculations to be uncoupled. A significant feature in the developed damage model is that a semi-coupled approach has been utilized in which a load in a

particular coordinate direction can result in a damage and stiffness reduction in multiple coordinate directions. This semi-coupled approach, while different from the methodology used in many existing damage mechanics models, has the potential to more accurately reflect the damage behavior that actually takes place, particularly for composites with more complex fiber architectures. As will be described later, the damage model has the capability to simulate the non-linear unloading present in composites before the peak stress is reached, and the post-peak stress degradation that can take place after the peak stress is reached. A wide variety of failure models, which can define the peak stress or designate the point after the peak stress where an element is to be eroded in a finite element analysis, have been developed for composites. In commonly used models such as the Tsai-Wu failure model [5], a quadratic function of the macroscopic stresses is defined in which the coefficients of the failure function are related to the tensile, compressive and shear failure stresses in the various coordinate directions. This model, while mathematically simple and easy to implement numerically, assumes that the composite failure surface has an ellipsoidal (in 2D) or ovoid (in 3D) shape. In reality, composite failure surfaces often are not in the form of simple shapes. In order to more accurately reflect the complex failure response observed in composites, a generalized tabulated failure model as well as a point cloud failure criterion has been developed in which the failure surface of the composite material can be input in a tabulated fashion.

2.1 Summary of Deformation Model

A complete description of the previously developed deformation model is given in [1] and [2]. A summary of the key features of the model is presented here. In the deformation model, a general quadratic three-dimensional orthotropic yield function based on the Tsai-Wu failure model is specified as follows, where 1, 2, and 3 refer to the principal material directions.

$$f(\sigma) = -1 + \begin{pmatrix} F_1 & F_2 & F_3 & 0 & 0 & 0 \end{pmatrix} \begin{pmatrix} \sigma_{11} \\ \sigma_{22} \\ \sigma_{33} \\ \sigma_{12} \\ \sigma_{23} \\ \sigma_{31} \end{pmatrix} + \begin{pmatrix} \sigma_{11} & \sigma_{22} & \sigma_{33} & \sigma_{12} & \sigma_{23} & \sigma_{31} \end{pmatrix} \begin{pmatrix} F_{11} & F_{12} & F_{13} & 0 & 0 & 0 \\ F_{12} & F_{22} & F_{23} & 0 & 0 & 0 \\ F_{13} & F_{23} & F_{33} & 0 & 0 & 0 \\ 0 & 0 & 0 & F_{44} & 0 & 0 \\ 0 & 0 & 0 & 0 & F_{55} & 0 \\ 0 & 0 & 0 & 0 & 0 & F_{66} \end{pmatrix} \begin{pmatrix} \sigma_{11} \\ \sigma_{22} \\ \sigma_{33} \\ \sigma_{12} \\ \sigma_{23} \\ \sigma_{31} \end{pmatrix} \tag{1}$$

In the yield function, σ_{ij} represents the stresses and F_{ij} and F_k are coefficients that vary based on the current values of the yield stresses in the various coordinate directions. By allowing the coefficients to vary, the yield surface evolution and hardening in each of the material directions can be precisely defined. The values of the normal and shear coefficients can be determined by simplifying the yield function for the case of unidirectional tensile and compressive loading in each of the coordinate directions along with shear tests in each of the shear directions. In Equation (1), the stresses are the current value of the yield stresses in the normal and shear directions. To determine the values of the off-axis coefficients (which are required to capture the stress interaction effects), the results from 45° off-axis tests in the various coordinate directions can be used. The values of the off-diagonal terms in the yield function can also be modified as required in order to ensure that the yield surface is convex [1,2]. A non-associative flow rule is used to compute the evolution of the components of plastic strain. The plastic potential, *h*, for the flow rule is shown in Equation (2)

$$h = \sqrt{H_{11}\sigma_{11}^2 + H_{22}\sigma_{22}^2 + H_{33}\sigma_{33}^2 + 2H_{12}\sigma_{11}\sigma_{22} + 2H_{23}\sigma_{22}\sigma_{33} + 2H_{31}\sigma_{33}\sigma_{11} + H_{44}\sigma_{12}^2 + H_{55}\sigma_{23}^2 + H_{66}\sigma_{31}^2} \tag{2}$$

where σ_{ij} are the current values of the stresses and H_{ij} are independent flow rule coefficients, which are assumed to remain constant. The values of the coefficients can be computed based on average plastic

Poisson's ratios [1,2]. Other trial and error or optimization methods can also be employed to estimate the values of the flow rule coefficients. The plastic potential function in Equation (2) is used in a flow law to compute the components of the plastic strain rate, where the usual normality hypothesis from classical plasticity [5] is assumed to apply and the variable $\dot{\lambda}$ is a scalar plastic multiplier. In the equation, $\boldsymbol{\sigma}$ is the stress vector and $\boldsymbol{\varepsilon}^p$ is the plastic strain vector. The dot above the variables indicates time derivatives.

$$\dot{\boldsymbol{\varepsilon}}^{p} = \dot{\lambda}\frac{\partial h}{\partial \boldsymbol{\sigma}} \tag{3}$$

Given the flow rule, the principal of the equivalence of plastic work [5] can be used to determine that the plastic potential function, *h*, can be defined as the effective stress and the plastic multiplier can be defined as the effective plastic strain.

To compute the current value of the yield stresses needed for the yield function, tabulated stress-strain curves are used to track the yield stress evolution. In the most general 3D case, a user is required to input twelve stress versus strain curves. Specifically, the required curves include uniaxial tension curves in each of the normal directions (1,2,3), uniaxial compression curves in each of the normal directions (1,2,3), shear stress-strain curves in each of the shear directions (1-2, 2-3 and 3-1), and 45° off-axis tension curves in each of the 1-2, 2-3 and 3-1 planes. The 45° curves properly capture the stress interaction effects in the yield function, as reflected in the F_{ij} terms in Equation (1) where $i \neq j$ such as F_{12}. For the case where plane stress simulations are conducted using thin shell elements, only an appropriately reduced set of input curves are required. Furthermore, the off-axis curves are not strictly required and can be omitted. Strain rate effects and thermal softening can be accounted for within the material model by inputting a full set of stress strain curves for a variety of strain rates and temperatures. By utilizing tabulated stress-strain curves to track the evolution of the deformation response, the experimental stress-strain response of the material can be better approximated. To track the evolution of the deformation response along each of the stress-strain curves, the effective plastic strain is chosen to be the tracking parameter. Using a numerical procedure based on the radial return method [5] in combination with an iterative approach, the effective plastic strain is computed for each time/load step. The stresses for each of the tabulated input curves corresponding to the current value of the effective plastic strain are then used to compute the yield function coefficients.

2.2 Summary of Damage Model

The deformation portion of the material model provides most of the capability of the model to simulate the nonlinear stress-strain response of the composite. However, to capture the nonlinear unloading often observed in composites [4], as well as post-peak stress degradation and stress softening, a complementary damage law is required. In the damage law formulation, previously developed and presented in [4], strain equivalence is assumed, in which for every time step the total, elastic, and plastic strains in the actual and effective stress spaces are the same [4]. The utilization of strain equivalence permits the plasticity and damage calculations to be uncoupled, as all of the plasticity computations can take place in the effective stress space.

The first step in the development of the damage model is to relate the actual stresses to a set of effective stresses by use of a damage matrix **M**

$$\boldsymbol{\sigma} = \mathbf{M}\boldsymbol{\sigma}_{eff} \tag{4}$$

In the equation, **M** is the damage matrix, $\boldsymbol{\sigma}$ is the stress vector in the actual, "damaged" stress space and $\boldsymbol{\sigma}_{\mathbf{eff}}$ is the stress vector in the "effective", "undamaged" stress space. The effective stress rate vector can be related to the total and plastic strain rate vectors by use of the standard elasto-plastic constitutive equation.

$$\dot{\boldsymbol{\sigma}}_{eff} = \mathbf{C}\left(\dot{\boldsymbol{\varepsilon}} - \dot{\boldsymbol{\varepsilon}}_{p}\right) \tag{5}$$

In the equationj, **C** is the standard elastic stiffness matrix, σ_{eff} is the "effective", "undamaged" stress vector, and ε is the total strain vector. Note that the actual total and plastic strain rate vectors are used due to the strain equivalence assumption.

In order to maintain a one-to-one relationship between the effective stresses and the actual stresses (i.e., to ensure that a uniaxial load in the actual stress space does not result in a multi-axial load in the effective stress space), the damage matrix is assumed to be diagonal. An implication of a diagonal damage matrix is that loading the composite in a particular coordinate direction only leads to a stiffness reduction in the direction of the load due to the formation of matrix cracks perpendicular to the direction of the load. However, as discussed in detail in [4], in composites, particularly those with complex fiber architectures, a load in one coordinate direction can lead to stiffness reductions in multiple coordinate directions. To maintain a diagonal damage tensor while still allowing for the damage interaction in at least a semi-coupled sense, each term in the diagonal damage matrix should be a function of the total and/or plastic strains in each of the normal and shear coordinate directions. Note that strains are chosen as the "tracking parameter" since, within the context of the developed formulation, the material nonlinearity during loading is simulated by use of a plasticity-based model. The strains therefore track the current state of load and deformation in the material.

To properly characterize the damage model in a tabulated fashion, each of the damage parameters can be determined as a function of the strain in a particular coordinate direction. For example, to characterize the damage response of a composite before the peak (maximum) stress is reached, for the case of loading in the 1 direction, a composite specimen must be loaded to a certain strain level in the 1 direction. The material is then unloaded to a state of zero stress, and then reloaded elastically in each of the coordinate directions to determine the reduced modulus of the material in each of the coordinate directions. This data can then be used to determine the values of the damage parameters for a particular value of strain. This process then needs to be repeated for multiple values of strain to determine a full tabulated characterization of the damage parameters as a function of strain.

The damage model has also been augmented to model the stress degradation that takes place after the peak stress in the stress-strain response is obtained. Accounting for this "post-peak stress degradation" permits the correct simulation of the additional deformation and energy absorption that takes place in an actual composite structure when loaded beyond the peak stress during an impact or dynamic crush event. An example of how the post-peak stress degradation can be represented in a shear stress-strain curve is shown in Figure 1. In this figure, after the peak stress is obtained the stress is degraded to a significantly lower equilibrium stress which is held constant until a defined effective strain is reached. As can be seen in the figure, this behavior is accounted for within MAT_213 by rapidly increasing a damage parameter to a defined high, constant, value once the peak stress is reached. Further details on the development and implementation of the ability to model the post-peak stress degradation can be found in Achstetter [6].

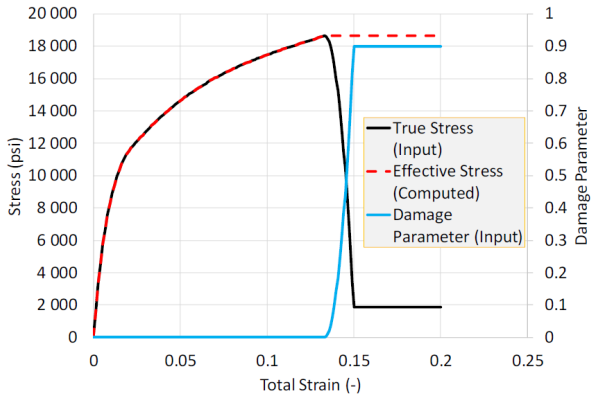

Fig.1: Input shear stress-strain curve for MAT_213 including stress degradation and damage curve.

2.3 Summary of Failure Model

As discussed earlier in this paper, the majority of the available failure models for composites utilize mathematical functions to describe the failure surface, which impose a specific shape on the failure surface. For example, the classical Tsai-Wu failure surface defines an elliptical shape for the two-dimensional failure surface in stress space. However, the failure surfaces of composites often do not exhibit this simple shape. Many actual failure surfaces cannot be easily defined by a mathematical function of the stresses. An alternative method to define a failure surface in a functional form suitable for implementation into a computer code while not enforcing a defined shape to the failure surface was developed and presented in [7]. In this failure model, known as the Generalized Tabulated Failure Criteria (GTFC), the failure surface is defined in a tabulated fashion. In this approach, a variable θ defines the relative location of the point on the failure surface in stress space, while a second variable *r* defines the "magnitude" of the failure surface point in the stress space location. The "magnitude" of the points on the failure surface are defined by using a stress invariant defined as follows for the plane stress case:

$$r = \sqrt{\sigma_{11}^2 + \sigma_{22}^2 + 2\sigma_{12}^2} \tag{6}$$

This invariant can be like a "radius" from the origin to the failure surface. The factor 2 in front of the shear stress term reflects the symmetry of the stress tensor. For the case of three-dimensional loading, a similar expression can be defined using the out-of-plane stresses, and the two expressions can be combined by using a "sum of squares" approach. Stresses or strains can be used in defining the dependent variable, making the model more general. In the current version of MAT213, the strain-based version of the "radius" invariant is more commonly used. Using an invariant type of term also allows for the stress (or strain) interactions to be more appropriately accounted for in the failure definition and helps to ensure that the failure definition will be accurate for a variety of loading conditions. This approach allows a failure surface with an arbitrary shape to be described using a single value function. For a realistic composite failure surface with an arbitrary shape, the relationship between "r" and "θ" cannot be easily defined by a closed-form mathematical function. As a result, a tabulated approach is employed for the current material model, where a series of "r" and "θ" pairs are explicitly defined for a given failure surface, which can provide an accurate representation of the failure surface. Particularly when used to define failure that occurs before the peak stress is reached, the tabulated approach allows for the use of experimentally defined failure surface data, a failure surface defined using any existing failure model, or a combination of experimental and numerically obtained "virtual" data. The combined approach can allow for the case where actual failure data are only available for a portion of the total stress space, with "virtual" data being required to fill in the gaps in the failure surface. However, since this failure model is often currently used to govern element erosion that takes place after the peak stress is reached, the use of experimental failure (i.e., peak stress) data may result in an excessively brittle material response. Ongoing work is investigating alternative means of defining the inputs for the failure model, and most work to date has assumed a constant failure strain.

3 Simulation of Crush Response of Structural Energy Absorber Concept

Research is currently being carried out at the NASA Langley Research Center which is looking into the development of lightweight energy absorbing structures to improve crashworthiness capabilities of rotorcraft structures. This work is looking specifically at improving crashworthiness in electric vertical takeoff and landing (eVTOL) designs which place a large emphasis on lightweight structural components. Previous research, including full scale helicopter crash tests to assess the dynamic response of transport-category rotorcraft under combined forward and vertical loading, identified a hybrid carbon-Kelvar® composite as a promising material for developing lightweight energy absorbing components [8]. This material is currently being evaluated in the design of crush tubes to reduce seat level accelerations and to reduce dynamic impact loads experienced by occupants.

The hybrid carbon-Kevlar® composite is a woven composite material where T300 3k carbon fiber tows are used in the warp direction and Kevlar 49 3k fiber tows are used in the fill direction. The matrix material is an Epon 828 epoxy with an Epicure 3223 hardener. A photo of the hybrid fabric is shown in Figure 2. A detailed test program, including a full suite of longitudinal and transverse tension, compression, and shear tests, was carried out by Slaughter et al. [9] to determine the fundamental mechanical response of the composite and to generate the data needed to fully populate a MAT_213 input deck.

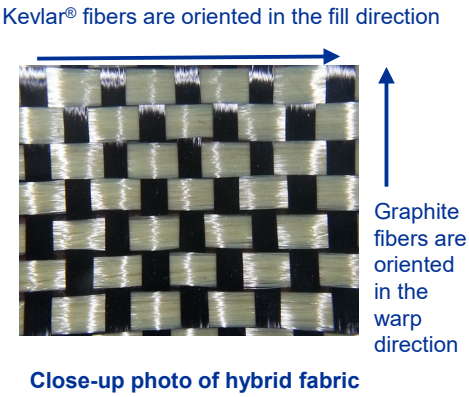

Fig.2: Woven carbon/Kevlar composite used in crush tube studies.

The crush tube design, generated using the hybrid composite material, is shown in Figure 3. The tube is composed of four layers of the hybrid composite material oriented 45° to vertical. To evaluate the energy absorbing capability of this design, drop tower testing was conducting in which a 105-lb. rigid mass was impacted into the crush tube at a velocity of 20 ft/s. In these tests the acceleration of the mass was recorded to assess the energy absorbing profile produced by the design. A representative model of this test setup was generated. The crush tube was modeled using quadrilateral shell elements with an element length of 0.1 in. The composite layup was defined using the *PART_COMPOSITE option within LS-DYNA. The impactor was modeled using solid elements with a rigid aluminum material with a defined initial velocity matching that measured at impact during the test. The crush tube impact model contained 17,872 elements and 20,108 nodes. The crush tube model impact model is shown in Figure 4.

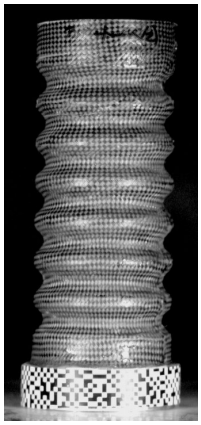

Fig.3: Composite crush tube of structural energy absorber material.

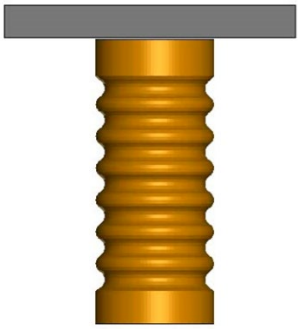

Fig.4: Composite crush tube model.

Simulations of the tube crushing response were conducted and the computed tube acceleration was compared to the experimental results. As a baseline, MAT_58 was also used (along with MAT_213) to simulate the crush tube response, as a MAT_58 characterization of the woven carbon/Kevlar material had been carried out under previous research [10,11]. The acceleration versus time response for a representative test is shown in Figure 5 along with the simulation results obtained by using MAT_58 and MAT_213. As can be seen in the figure, the results obtained using MAT_58 compared favorably to the experimental response. Initially, the SLIM and ERODS parameters used for the MAT_58 analyses were used to characterize the post peak stress damage (stress degradation) and failure model (element erosion) parameters for the MAT_213 simulations. However, these initial characterizations yielded non-optimal results. An independent correlation of the damage and failure model parameters for MAT_213 was then carried out to improve the accuracy of the simulations. As can be seen in the figure, by adjusting the MAT_213 damage and failure model parameters an acceptable correlation with the experimental results was obtained, and an improved correlation with the experimental results at the time of initial contact (as compared to MAT_58) was obtained. On a conceptual level, there are strong synergies between the SLIM and ERODS parameters in MAT_58 and the methods used in MAT_213 to compute the post-peak stress damage and failure model parameters.

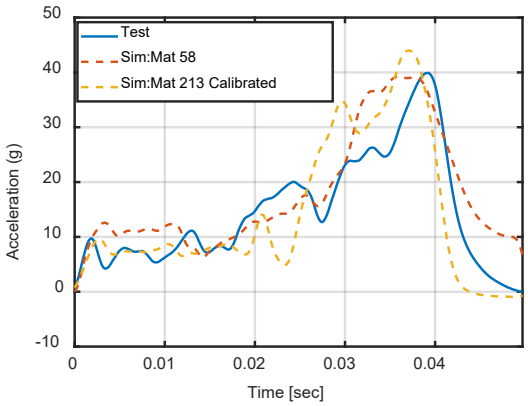

Fig.5: Crush tube acceleration versus time predictions using MAT_58 and MAT_213 with comparison to an experimental result.

To further explore the effects of the various deformation and damage model parameters on the crush tube simulation results obtained using MAT_213, the damage model parameters and the flow rule coefficients were varied, and a series of simulations were carried out. Note that unlike the results shown in Figure 5, where the MAT_213 parameters were calibrated to obtain an optimal match with the experimental results, for these studies initial characterized values for the MAT_213 damage and failure parameters were used. In Figure 6, results obtained by varying the damage model parameters controlling the level of stress degradation in tension after the peak stress was reached are plotted. All other damage parameters were maintained at a constant value. A lower level of damage indicates higher levels of (constant) stress after the peak stress is reached varied to account for varying levels of stress degradation after the peak stress was reached. For example, a damage value of 0.3 indicates that after the peak stress is reached the level of stress is reduced to a value equal to 70% of the peak stress and held constant. As can be seen in the figure, changing the level of damage significantly affected the peak acceleration, with lower levels of damage providing improved correlations to the experimental results. In Figure 7, simulations conducted where the ratio of the shear plasticity flow rule coefficient (H_{44}) to the transverse normal plasticity flow rule coefficient (H_{22}) were varied are shown. As can be seen in this figure, lower values for the shear flow rule coefficient resulted in improved predictions compared to the results obtained by using higher values of H_{44}.

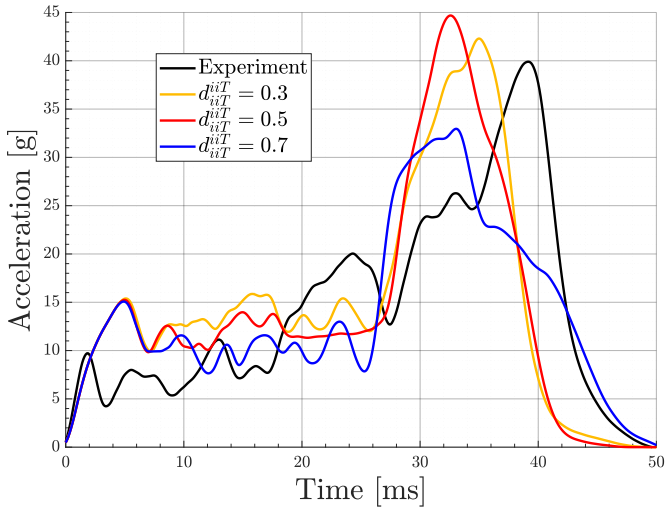

Fig.6: Crush tube acceleration versus time predictions using MAT_213 with varying levels of stress degradation after the peak stress is reached.

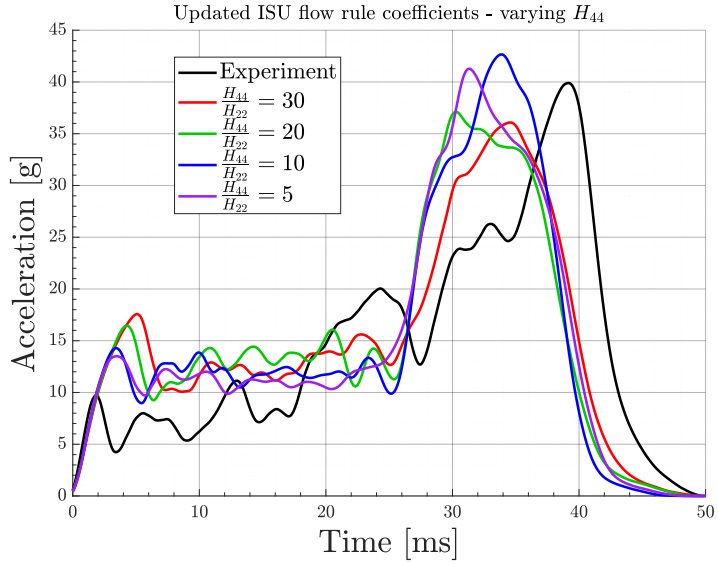

Fig.7: Crush tube acceleration versus time predictions using MAT_213 with varying levels of ratio of shear plasticity flow rule coefficient to transverse normal plasticity flow rule coefficient.

4 Simulation of Ballistic Impact Response of Material Used for Rotorcraft Fuselage Structure

Under the research program being carried out at the NASA Langley Research Center to examine the crashworthiness capabilities of rotorcraft structures subjected to impact conditions, composite fuselage structures composed of a woven composite with carbon fibers in both the warp and fill direction have been examined. These composites are plane weave woven composites with 3K70PW carbon fibers and an INF14 epoxy matrix. A detailed test program, including a full suite of longitudinal and transverse tension, compression, and shear tests, was carried out by Keshavanarayana et al. [12] to determine the fundamental mechanical response of the composite and to generate the data needed to fully populate a MAT_213 input deck.

An additional area of interest for these fuselage structures is examining their ability to withstand a bird strike event. As part of this effort, simulation studies are underway in which an artificial bird model is being developed for use within LS-DYNA impact analyses. As a first step in this process, a MAT_213

card for the woven composite has been developed and simulation studies of the impact of an aluminum projectile on a composite plate have been conducted. Experimentally, a series of dynamic impact tests on flat plates made of the woven composite were performed at NASA Glenn Research Center in accordance with ASTM D8101/D8101M-1732 [13]. The projectile was a hollowed-out cylinder with a hemispherical nose as shown in Figure 8. The projectile was made of Aluminum 6061 with a nominal mass of 0.11 lb. The composite plate was a rectangular plate with a nominal length and width of 12 in. A 40 ply composite with a laminate orientation of $[45/0/-45/90/90/-45/0/45]_s$ was used. The plate was held in place by being bolted to a circular clamp with a nominal inner diameter of 10 in fastened with 28 bolts through the specimen to a massive rear plate with a hole of the same diameter. High speed digital image correlation (DIC) was used to accurately measure the backside displacement of the plate during impact. A single stage gas gun was used to propel the projectile such that it impacted the plate in the normal direction nominally at the center of the plate. For the specific test to be described here, the plate was impacted at a velocity of 126.5 ft/s. For this test, the projectile did not penetrate the plate and rebounded with a velocity of 80.16 ft/s. A photo of a typical plate used in the impact tests is shown in Figure 9.

Fig.8: Projectile used in impact tests.

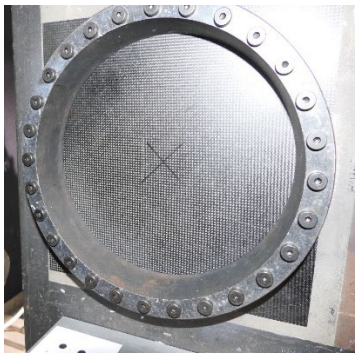

Fig.9: Composite plate used in impact tests.

Boundary conditions, element size, and projectile geometry for the impact simulations were kept consistent with previous work by Ricks et al. [14]. The plate was modeled using shell elements, and appropriate boundary conditions were applied to simulate constraints due to the fixture. The geometry of the plate and projectile is shown in Figure 10. The projectile was modeled using a piecewise linear plasticity model with standard Aluminum 2024 properties. The MAT_213 input for the composite plate was developed using the data obtained by Keshavanarayana et al. [12].

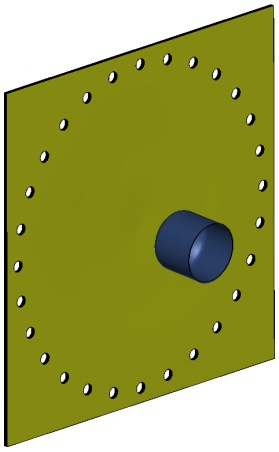

Fig.10: Geometry of the plate and projectile used for impact simulations.

As an example of the types of validation results that were obtained, Figure 11 shows the experimental and simulated backside out-of-plane displacements as a function of time at the center of impact predicted for the case described above, where the projectile impact velocity was low enough that the projectile rebounded after impact. The simulated displacements corresponded closely to what was observed experimentally. In addition, a rebound velocity of 84.36 ft/s was predicted, which is within six percent of the experimental rebound velocity.

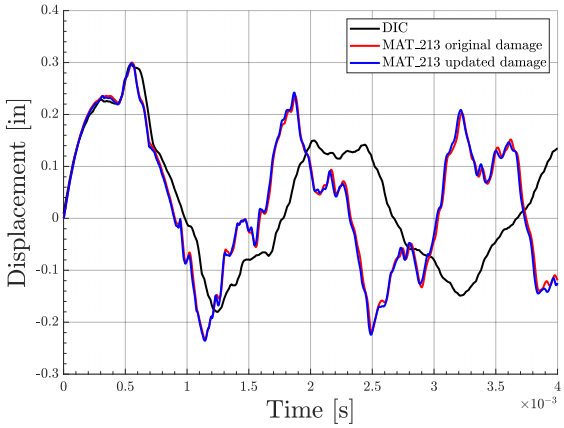

Fig.11: Backside out-of-plane displacement at the center of impact as a function of time for case with impact velocity of 126.5 ft/s.

5 Simulation of Impact Response of Thermoplastic Matrix Composites

An additional area of interest at NASA is developing the ability to simulate the dynamic and impact response of thermoplastic matrix composite materials. Thermoplastic matrix composites can have increased ductility and strain rate dependence as compared to traditional epoxy matrix composites. As a result, these materials have the potential to provide improved performance under dynamic loading conditions. Examining the ability of MAT_213 to appropriately simulate the dynamic response of thermoplastic matrix composites is therefore of interest.

One set of studies involved simulating the ballistic impact response of an IM7/PEKK composite with a $[+45/0/-45/90]_{2s}$ laminate layup. The material properties used for the IM7/PEKK composite and the development of the MAT_213 input parameters are described in Buenrostro et al [15]. Experimentally, a series of dynamic impact tests on flat plates made of the unidirectional composite were once again performed at NASA Glenn Research Center in accordance with ASTM D8101/D8101M-1732 [13], with the exception that a 0.2 lb projectile was used, which is a deviation from the standard. The simulations of two specific impact tests are described here. For the first impact test the impact velocity was 60 ft/s.

For this test, the projectile did not penetrate the impacted plate and minimal damage occurred. An additional test conducted at an impact velocity of 475 ft/s was also simulated. For this test, the projectile also did not penetrate the plate, but a significant amount of delamination of the composite plate was observed. A detailed description of the test procedures and test results are also described in Buenrostro et al. [15].

To simulate the impact tests, a finite element model of the composite plate and projectile was developed where thin shell elements were used to model the composite plate. Similar to what was done for impact simulations described earlier in this paper, the boundary conditions, element size, and projectile geometry for the impact simulations were kept consistent with previous work by Ricks et al. [14]. Tiebreak contact elements were used to simulate the delamination behavior between the composite plies using methods described in detail in Buenrostro et al. [15]. One significant improvement that was carried out for these simulations is that a “fiber aligned” mesh was used for each layer of the composite plate. In this type of modeling approach, the finite element mesh is aligned along the fiber direction of the material for each ply. This type of approach has been found to improve the accuracy of the dynamic simulations. A diagram of the finite element model for the ballistic impact simulations, including the boundary conditions, is shown in Figure 12. In this figure, examples of the fiber aligned meshing are also shown.

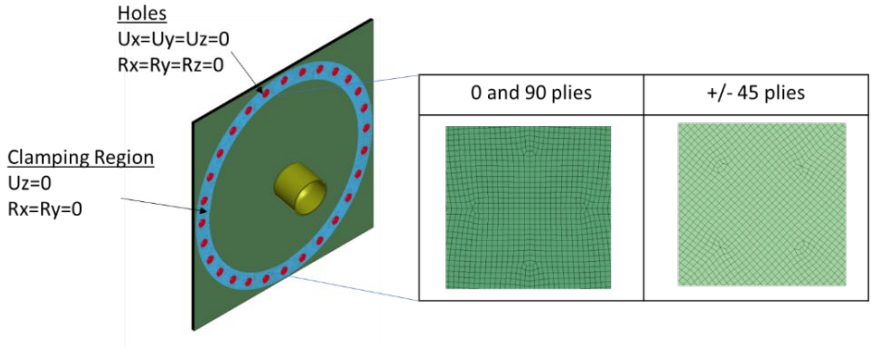

Fig.12: Illustration of fiber aligned meshing and boundary conditions for ballistic impact simulations of IM7/PEKK composite.

Figure 13 shows the experimental and simulated backside displacement measured at the center of impact for the test with an impact velocity of 60 ft/s. For this simulation, the first peak was accurately captured, and while not shown here the model captured the projectile rebound well. Deviations between the simulation response and the experiment were seen in subsequent peak deflections which could be due to a simplification of the boundary conditions. Figure 14 shows a comparison between the experimental and predicted levels of delamination for the ballistic test with an impact velocity of 475 ft/s. While a large amount of delamination was predicted by the simulation, the amount and range of the delamination that was computed was underpredicted compared to the experimental results. Future efforts will involve developing methods to improve the ability of simulations to accurately predict the level of delamination in higher velocity impact tests.

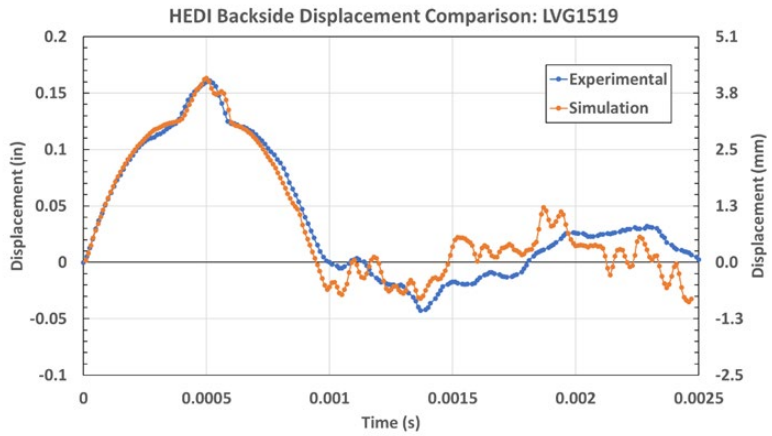

Fig.13: Experimental and computed backside displacement at the panel center from an impact test of the IM7/PEKK composite laminate with an impact velocity of 60 ft/s.

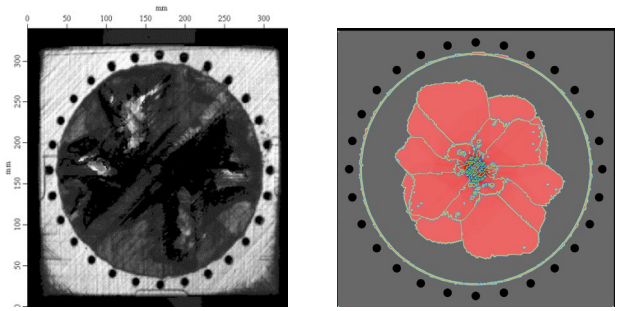

Fig.14: Comparison of post-test non-destructive evaluation image (left) which shows no damage in light gray and damage in black, and predicted simulation damage (right) which shows no damage in gray and damage in red for an impact test of the IM7/PEKK composite with an impact velocity of 475 ft/s

6 Conclusions

A generalized composite model suitable for use in polymer composite impact simulations has been developed. The model utilizes a plasticity-based deformation model based on generalizing the Tsai-Wu failure criteria. A strain equivalent damage model has also been developed in which loading the material in a particular coordinate direction can lead to damage in multiple coordinate directions. A tabulated failure model has been developed which facilitates the use of actual composite failure data in an analysis. This material model has been successfully implemented within the commercial transient dynamic finite element code LS-DYNA as MAT_213. Initial simulation results have indicated the model has a strong potential to simulate the dynamic response of composite materials for multiple applications of interest to NASA.

There are several areas of future work identified that will be addressed in ongoing efforts. First, improved methods of characterizing plasticity parameters and post-peak damage and failure response are being developed in order to allow the characterization to take place using the result of coupon level and other small-scale tests to limit the need to calibrate the material parameters based on the results of large scale structural simulations. Improved methods to simulate the interply delamination are being developed. Given the fact that strain rate and temperature effects can be significant in composites when subjected to dynamic loads, additional simulations will be conducted to more rigorously account for these effects in the analyses. Expanded investigations will be conducted into the use of MAT_213 for the analysis of various additional impact, crush, and crash projects of interest to NASA.

7 Acknowledgements

The authors wish to thank the NASA Hi-Rate Composite Manufacturing Project (HiCAM) and the NASA Revolutionary Vertical Lift Technology Project (RVLT) for sponsoring the research presented in this paper. The authors would additionally like to thank the Office of Naval Research for sponsoring the work on the impact simulation of the IM7/PEKK composites presented in this paper. The authors would like to thank Dr. Mike Pereira, Duane Revilock and Charles Ruggeri of the NASA Glenn Ballistic Impact Lab for providing the ballistic impact experimental results shown in this paper. Dr. Ashraf Bastawros of Iowa State University is thanked for providing additional support for the research efforts of author Daniel Slaughter.

8 Summary

A material model has been developed which incorporates several key capabilities which have been identified as lacking in currently available composite impact models. The material model utilizes experimentally based tabulated input to define the evolution of plasticity and damage as opposed to specifying discrete input parameters (such as modulus and strength). The material model has been implemented into LS-DYNA as MAT_213. The model can simulate the nonlinear deformation, damage and failure that takes place in a composite under dynamic loading conditions. The deformation model utilizes an orthotropic plasticity formulation. For the damage model, the nonlinear unloading response that is observed prior to the point where the peak stress is reached can be simulated, as well as the stress degradation response that occurs after the peak stress is reached. A variety of failure models, including a generalized tabulated failure model which facilitates the utilization of general failure surfaces, have been implemented into MAT_213. Recent studies at NASA have concentrated on using MAT_213 to analyze both the impact and crush response of a variety of laminated and textile architectures. Several of these studies were discussed in the paper. For example, a woven carbon/Kevlar composite is currently being examined for use in an energy absorber system for rotorcraft structures. MAT_213 analyses have been conducted to examine the ability of the model to accurately simulate the dynamic crush response of this material. Studies were also conducted to examine the ability of MAT_213 to simulate the ballistic impact response of representative thermoplastic and thermoset matrix composites.

9 Literature

[1] Goldberg, R., Carney, K., DuBois, P., Hoffarth, C., Harrington, J., Rajan, S., and Blankenhorn, G.: “Development of an Orthotropic Elasto-Plastic Generalized Composite Material Model Suitable for Impact Problems,” Journal of Aerospace Engineering, 2015, 10.1061/(ASCE)AS.1943-5525.000058004015083.

[2] Hoffarth, C.; Khaled, B.; Shyamsunder, L.; Rajan, S.; Goldberg, R.K.; Carney, K.S.; DuBois, P.; and Blankenhorn, G: “Verification and Validation of a Three-Dimensional Orthotropic Plasticity Constitutive Model Using a Unidirectional Composite”, Fibers, Vol. 5, Issue 1, 2017

[3] Daniel, I.M., and Ishai, O.: 2006. Engineering Mechanics of Composite Materials Second Edition. Oxford University Press, New York, 2006.

[4] Goldberg, R., Carney, K., DuBois, P., Hoffarth, C., Khaled, B., Rajan, S., and Blankenhorn, G.: “Analysis and Characterization of Damage Using a Generalized Composite Material Model Suitable for Impact Problems,” Journal of Aerospace Engineering, 2018,10.1061/(ASCE)AS.1943-5525.0000854.

[5] Khan, A.S., and Huang, S.: Continuum Theory of Plasticity. John Wiley and Sons, New York, 1995.

[6] Achstetter, T.: “Development of a Composite Material Shell-Element Model for Automotive Impact Applications.” PhD Dissertation, George Mason University, Fairfax, VA., 2019.

[7] Goldberg, R., Carney, K., DuBois, P., Hoffarth, C., Harrington, J., Shyamsunder, L., Rajan, S., and Blankenhorn, G.: “Implementation of a tabulated failure model into a generalized composite material model,” Journal of Composite Materials, Vol. 52, pp. 3445–3460, 2018.

[8] Littell J. D., Jackson K. E., Annett M. S., Seal M. D., and Fasanella E. L.: “The Development of Two Composite Energy Absorbers for Use in a Transport Rotorcraft Airframe Crash Testbed (TRACT 2) Full-Scale Crash Test,” Proceedings of the 71st Annual American Helicopter Society Forum, Virginia Beach, VA, May 5-7, 2015.

[9] Slaughter, D.M., Lee, H.-J., Goldberg, R.K., and Bastawros, A.F.: “Experimental Calibration of Flow Rule Coefficients for LS-DYNA MAT_213”, Proceedings of the 2024 International LS-DYNA User Conference, Plymouth, Michigan, October 22-23, 2024.

[10] Jackson K. E., Fasanella E. L., and Littell J.D.: “Development of a Continuum Damage Mechanics Material Model of a Graphite-Kevlar® Hybrid Fabric for Simulating the Impact Response of Energy Absorbing Subfloor Concepts,” Proceedings of the 73rd Annual AHS Forum, Ft. Worth, Texas, May 9-11, 2017.

[11] Putnam, J.B., Littell, J.D.: “Simulation and Analysis of NASA Lift Plus Cruise eVTOL Crash Test,” Proceedings from the Vertical Flight Society 79th Annual Forum and Technology Display, West Palm Beach, Florida, May 16-18, 2023.

[12] Keshavanarayana, S., Jagadheeswaran, S., and Yerram, G.: “In-plane Elasto-plastic characterization of 3K70PW Carbon Fabric/INF14 for MAT 213 material model,” Proceedings of the ASCE Earth and Space 2024 Conference, Miami, Florida, April 16-18, 2024.

[13] D30 Committee: “ASTM D8101/D8101M-18 Standard Test Method for Measuring the Penetration Resistance of Composite Materials to Impact by a Blunt Projectile”. ASTM International, 2018.

[14] Ricks, T.M., Goldberg, R.K., and Pereira, J.M.: “High-Energy Dynamic Impact Modeling of an AS4D/PEKK-FC Composite Using LS-DYNA MAT_213”, Proceedings of the 38th American Society for Composites Technical Conference, Woburn, Massachusetts, September 18-20, 2023.

[15] Buenrostro, J., Ricks, T.M., Miller, S., Revilock, D.M., Maurya, A., and Rajan, S.: “Simulating High Energy Dynamic Impact of IM7/PEKK Continuous Fiber Laminated Thermoplastic Composite using Notched Coupon Experiments,” Proceedings of the 39th American Society for Composites Technical Conference, San Diego, California, October 21-23, 2024.